

## Recent advances of polar transition-metal sulfides host materials for advanced lithium–sulfur batteries

Liping Chen\*, Xifei Li<sup>\*,§</sup> and Yunhua Xu<sup>†,‡,¶</sup>

*\*Institute of Advanced Electrochemical Energy and  
 School of Materials Science and Engineering*

*Xi'an University of Technology, Xi'an 710048, P. R. China*

*†Collaborative Innovation Center of Modern Equipment and Green Manufacturing  
 Xi'an University of Technology, Xi'an 710048, P. R. China*

*‡Yulin University, 4 Chongwen Road, Yulin, Shaanxi 719000, P. R. China*

*§xfli2011@hotmail.com*

*¶xuyunhua@vip.163.com*

Received 25 July 2018; Accepted 12 September 2018; Published 13 November 2018

Lithium sulfur batteries (LSBs) have been one of the most promising second batteries for energy storage. However, the commercialization of LSBs is still hindered by low sulfur utilization and poor cycling stability, resulting from shuttle effect and low redox kinetics of lithium polysulfides (LiPSs). Significant progress has been made over the years in enhancing the batteries performances and tap density with the transition-metal sulfides as sulfur host or additive in LSBs. In this review, we present the recent advances in the use of various nanostructured transition-metal sulfides applied in LSBs, and also focus on the interaction mechanisms of polar transition-metal sulfides with LiPSs and its catalysis for the redox of LiPSs. It may provide avenues for the application of transition-metal sulfides in LSBs. The challenges and perspectives of transition-metal sulfides are also addressed.

**Keywords:** Lithium sulfur batteries; transition-metal sulfides; shuttle effect; redox kinetic.

### 1. Introduction

Lithium sulfur batteries (LSBs) hold great prospect to meet the increasing need of advanced energy storage in battery field, owing to their high theoretical specific capacity ( $1675 \text{ mAh g}^{-1}$ ), low cost, and environmental friendliness.<sup>1–3</sup> However, the application of LSBs has been challenged by several obstacles, particularly low active material utilization and poor cycling stability. It may be due to the poor electronic conductivity of sulfur and its discharge end product  $\text{Li}_2\text{S}$ , the shuttle effect of the dissolved intermediates lithium polysulfides (LiPSs), and the large and repeated volume change.<sup>4</sup> Among these issues, the shuttle effect results in low utilization of sulfur, low Coulombic efficiency, and capacity decay, as well as anode corrosion,<sup>5</sup> which is the most thorny problem that leads to capacity decay.<sup>6,7</sup> Tremendous strategies have been proposed to retard the shuttle effect through using carbon materials as the sulfur host,<sup>8,9</sup> modification of the separator,<sup>10,11</sup> even designing interlayer or cathode coating.<sup>12,13</sup> However, non-polar carbon materials only show

limited anchoring sites for LiPSs and weak interaction between them, eventually leading to poor battery performance.<sup>5,14</sup> In recent years, the concept of using polar conductive materials for immobilizing sulfur and LiPSs by strong chemical bonding is an acknowledged strategy to suppress the diffusion of LiPSs and enhance the sulfur utilization.<sup>7,15</sup> In this concern, functionalized carbon materials, functional conductive polymers, and transition metal compounds, including oxide, sulfides, carbides, nitride, hydroxides and metal organic frameworks with abundant adsorption sites are regarded as promising sulfur hosts to chemically adsorb LiPSs for improving cathode performance.<sup>5,15–17</sup> Moreover, several studies have shown that accelerating the conversion kinetics of the LiPSs to  $\text{Li}_2\text{S}_2/\text{Li}_2\text{S}$ , and vice versa, is a promising way to mitigate the LiPSs shuttling.<sup>18,19</sup> In this concern, transition-metal sulfides (MSs,  $\text{M} = \text{Mo}, \text{Co}, \text{Ti}, \text{Ni}, \text{Fe}, \text{Cu}, \text{Mn}, \text{V}, \text{W}$  and  $\text{Zr}$ ) show great promise as a kind of sulfur host benefitting from their strong chemical interaction with sulfur species, triggering extensive attention and researches for LSBs. As demonstrated in Fig. 1, transition-metal sulfides not only possess strong chemical

<sup>§</sup>Corresponding author.

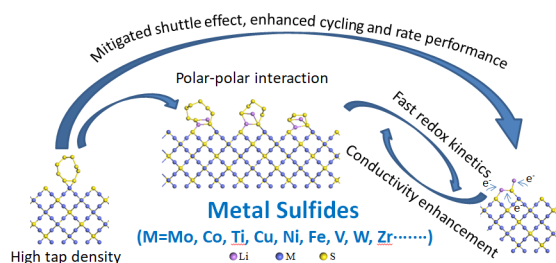


Fig. 1. Schematic illustration of the positive effect of transition-metal sulfides as sulfur host applied in LSBs.

affinity with LiPSs due to their large polar surface, but also reveal high catalytic activity to promote the redox kinetics of sulfur species, potentially suppressing the LiPSs shuttle.<sup>18</sup> Additionally, transition-metal sulfides themselves also possess high conductivity, which can enhance the conductivity of sulfur cathode when kept in contact with sulfur. Last but not least, the high density of transition-metal sulfides endows sulfur cathode high tap density, which benefits the volume energy density of LSBs.<sup>17,20</sup>

Here, recent advances of transition-metal sulfides applied in LSBs are reviewed, including polar-polar interaction of transition-metal sulfides with LiPSs/Li<sub>2</sub>S, conductivity enhancement, catalytic effect on the redox of sulfur species, sulfur-equivalent cathode or co-cathode material and tap density improvement, and its mechanisms are systematically discussed.

## 2. Positive Role of Sulfides in LSBs

### 2.1. Polar-polar interaction of transition-metal sulfides with LiPSs/Li<sub>2</sub>S

Transition-metal sulfides are usually utilized as host materials as well as interlayer for polysulfide adsorption in LSBs due to the strong bonds between metal sulfides and LiPSs/Li<sub>2</sub>S. The binding energy between sulfides and LiPSs/Li<sub>2</sub>S are much higher than that of graphite or graphene. As shown in Table 1, the binding energy of Li<sub>2</sub>S<sub>2</sub> and graphite is 0.28 eV, while that of TiS<sub>2</sub> and Li<sub>2</sub>S reaches 2.99 eV.<sup>15</sup> More importantly, the value of Li<sub>2</sub>S<sub>2</sub> and Co<sub>9</sub>S<sub>8</sub> is even up to 6.06 eV, which is the highest binding energy reported for lithium sulfide.<sup>21</sup> Additionally, the metal sulfides can also provide chemical interaction with non-polar sulfur, thus suppressing the dissolution of sulfur. For example, the binding energy can be up to 1.09 eV between Ni<sub>3</sub>S<sub>2</sub> and S<sub>8</sub>,<sup>22</sup> which is much higher than that of graphene (0.30 eV) and graphene with hydroxyl (0.47 eV).<sup>23</sup> The effect of the interaction can be visually observed by adsorption tests, that is, LiPSs solution gradually becomes lighter or colorless after the sulfides immersed.<sup>24,25</sup> For example, NiS exhibits strong adsorption capability for LiPSs, as shown in Fig. 2(a). The slight shift of

Table 1. Binding energies of LiPSs and different metal sulfides.

MSs	Crystal face	LiPSs molecules	Binding energies (eV)	Ref.
CoS <sub>2</sub>	(111)	Li <sub>2</sub> S <sub>4</sub>	1.97	19
Co <sub>3</sub> S <sub>4</sub>	(111)	Li <sub>2</sub> S <sub>4</sub>	2.26	24
		Li <sub>2</sub> S <sub>6</sub>	1.61	
		Li <sub>2</sub> S <sub>8</sub>	1.68	
	(220)	Li <sub>2</sub> S <sub>4</sub>	2.76	
		Li <sub>2</sub> S <sub>6</sub>	2.18	
		Li <sub>2</sub> S <sub>8</sub>	2.18	
Co <sub>9</sub> S <sub>8</sub>	(002)	Li <sub>2</sub> S <sub>2</sub>	2.26	21
	(202)		3.29	
	(008)		6.06	
	(002)	Li <sub>2</sub> S	2.74	
	(202)		3.41	
	(008)		3.96	
	(002)	Li <sub>2</sub> S <sub>4</sub>	1.71	
	(202)		1.56	
	(008)		4.10	
TiS <sub>2</sub>	—	Li <sub>2</sub> S	2.99	37
ZrS <sub>2</sub>	—		2.70	
VS <sub>2</sub>	—		2.94	
NiS <sub>2</sub>	(111)	Li <sub>2</sub> S <sub>4</sub>	2.06	34
(NiS <sub>2</sub> ) <sub>0.6</sub> (FeS) <sub>0.4</sub>	(001)	Li <sub>2</sub> S <sub>2</sub>	1.92	42
Ni <sub>3</sub> S <sub>2</sub>	(110)	S <sub>8</sub>	1.09	22
		Li <sub>2</sub> S <sub>8</sub>	1.92	
		Li <sub>2</sub> S <sub>6</sub>	2.15	
		Li <sub>2</sub> S <sub>4</sub>	2.29	
		Li <sub>2</sub> S <sub>2</sub>	3.90	
		Li <sub>2</sub> S	4.89	
Ni <sub>3</sub> S <sub>2</sub>	—	Li <sub>2</sub> S <sub>6</sub>	0.72	28
SnS <sub>2</sub>	—		0.80	
FeS	—		0.87	
CoS <sub>2</sub>	—		1.01	
VS <sub>2</sub>	—		1.04	
TiS <sub>2</sub>	—		1.02	
graphite	—	Li <sub>2</sub> S <sub>2</sub>	0.28	21
graphene	—	Li <sub>2</sub> S <sub>4</sub>	0.34	19

the Raman spectra peaks as well as the XPS speaks further confirms the electrons transfer from S<sub>x</sub><sup>2-</sup> to Ni<sup>2+</sup>, and the strong chemical interaction of Ni<sup>2+</sup> in NiS with S<sub>x</sub><sup>2-</sup> in Li<sub>2</sub>S<sub>x</sub>.<sup>26</sup> Additionally, the sulfides possess coupled interaction with Li<sub>2</sub>S<sub>n</sub> through S<sub>n</sub><sup>2-</sup>-M<sup>δ+</sup> and Li<sup>+</sup>-S<sup>δ-</sup> (of metal sulfides) binding.<sup>19,21,26</sup> The high affinity between sulfides and LiPSs mitigates its dissolution and improves the cycling stability of the sulfur cathodes. For example, the cycling performance of LSBs was visibly improved with CoS<sub>2</sub> anchored on carbon paper as the interlayer, due to the trap ability of CoS<sub>2</sub> for the LiPSs by forming strong chemical interaction.<sup>27</sup> Compared with original carbon aerogel/S electrode, the initial specific capacity of sulfur cathode increased from 1156 mAh g<sup>-1</sup> to 1343 mAh g<sup>-1</sup> when MoS<sub>2</sub> (8% molar ratio) was introduced, and better stability was obtained, due to the immobilizing effect of sulfur by MoS<sub>2</sub>.<sup>29</sup> In addition, Co<sub>3</sub>S<sub>4</sub>,<sup>24</sup> MoS<sub>2</sub>,<sup>29</sup> Co<sub>9</sub>S<sub>8</sub>,<sup>30</sup> TiS<sub>2</sub>,<sup>28</sup> SnS<sub>2</sub>,<sup>31</sup> Cu<sub>2</sub>S/CuS,<sup>32</sup> FeS<sub>2</sub>,<sup>33</sup> NiS<sub>2</sub>,<sup>34</sup> WS<sub>2</sub>,<sup>35</sup> VS<sub>2</sub>,<sup>36</sup> ZrS<sub>2</sub>,<sup>37</sup> etc., are all

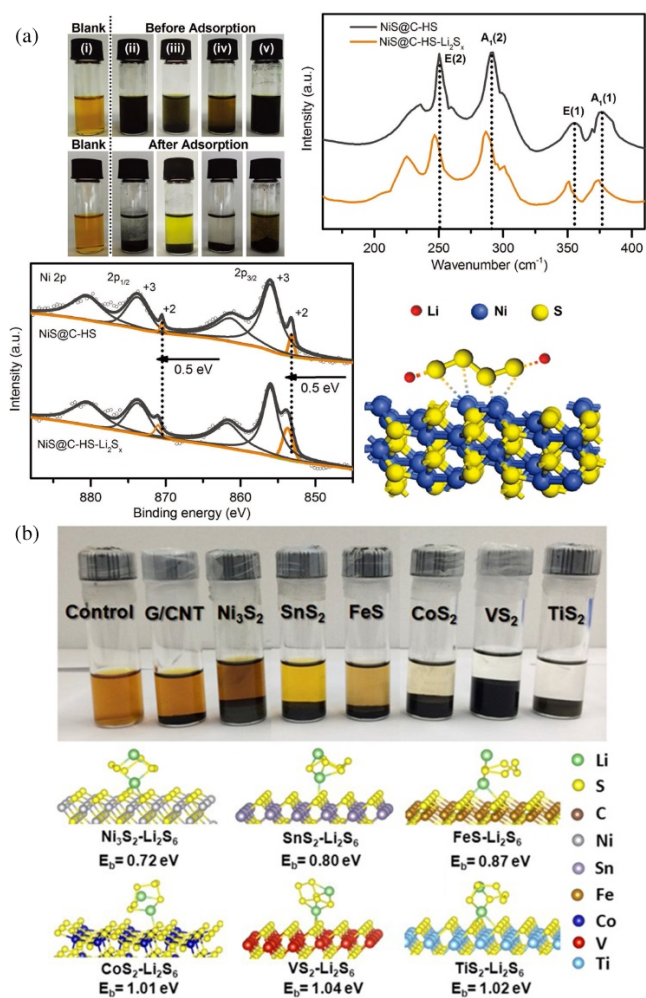


Fig. 2. (a) Photograph of (i) pristine LiPSs solution, the LiPSs solution before and after adsorbed by (ii) NiS@C-HS, (iii) C-HS@NiS, (iv) NiS@HS, and (v) C-HS; Raman and XPS spectra of Ni 2p of NiS@C-HS and NiS@C-HS-Li<sub>2</sub>S<sub>4</sub>; and schematic illustration of the Li<sub>2</sub>S<sub>4</sub> binding configuration with NiS.<sup>26</sup> (b) Digital image of the adsorbed Li<sub>2</sub>S<sub>6</sub> by carbon and Ni<sub>3</sub>S<sub>2</sub>, SnS<sub>2</sub>, FeS, CoS<sub>2</sub>, VS<sub>2</sub> and TiS<sub>2</sub>, and simulation of Li<sub>2</sub>S<sub>6</sub> interacts with these sulfides: atomic conformations and binding energies.<sup>28</sup>

capable of absorbing LiPSs. The chemical interaction is dominated by the bond of the Li<sup>+</sup> of LiPSs and the sulfur ion of the sulfide, and the larger binding energy, the stronger interactions, thus the better anchoring effect,<sup>28</sup> as shown in Fig. 2(b). However, binding free energy ( $\Delta G_B$ ) is much more valuable to evaluate the interaction strength between cathode material and sulfur species because it possesses the advantage of involving thermal and entropy corrections.<sup>38</sup> Moreover, the adsorption energy ( $E_a$ ) between metal sulfides and Li<sub>2</sub>S<sub>x</sub>/S<sub>8</sub> was also conducted to evaluate the chemisorption capability.<sup>39</sup>

It is noted that the strong interaction also facilitates the formation of Li<sub>2</sub>S. Compared to bare graphene, CoS<sub>2</sub> favor the controllable nucleation and growth of Li<sub>2</sub>S.<sup>19</sup> Furthermore, relieved shuttle accordingly remits the corrosion of Li anode. MoS<sub>2</sub>/graphene interlayer was designed to restrain the

shuttle effect with the synergistic effect of physical and chemical adsorption. As a result, the cycled Li anode exhibited uniform and lower roughness of surface with the addition of MoS<sub>2</sub>/graphene interlayer, due to the relieved dissolution of LiPSs to the electrolyte.<sup>40</sup> The strong interaction relieves the shuttle of LiPSs, which promotes the cycling stability. However, the chemical interaction is not the only critical factor for trapping LiPSs. Therefore, only the binding energy or/and binding free energy (adsorption energy) may not be the sole evaluation criteria to select the best one among these metal sulfides for performance improvement.

In addition to types of sulfides, crystal structure may affect the capacity of trapping LiPSs. This is because different crystal planes possess various adsorption energies<sup>39</sup> or binding energies<sup>24</sup> with different LiPSs molecules (Li<sub>2</sub>S<sub>2</sub>, Li<sub>2</sub>S<sub>4</sub>, Li<sub>2</sub>S<sub>6</sub> and Li<sub>2</sub>S<sub>8</sub>). The binding energies between LiPSs and different sulfides with different crystal planes are summarized in Table 1. Consequently, sulfides should be designed with controlled crystal structure, or two different kinds of sulfides with synergistic effect for different LiPSs molecules should be composited, to maximize the interaction on different LiPSs molecules. It is noted that different crystal planes possess various binding energies for Co<sub>9</sub>S<sub>8</sub>. Additionally, the binding energy between Li<sub>2</sub>S and sulfides is site-dependent, which is different in terrace and edge sites. The Mo-edge and S-edge of MoS<sub>2</sub> exhibit binding energy with Li<sub>2</sub>S up to 4.48 and 2.70 eV, respectively, which are much higher than that of terrace sites (0.87 eV) of MoS<sub>2</sub>.<sup>41</sup> The edges facilitate uniform distribution of Li<sub>2</sub>S and prevent its accumulation, as a result, the sample with most edge sites delivers higher discharge capacity, cycling stability as well as rate performance than the one with terrace sites. This guides the structure design to improve cathode performance by exposing more edge sites on the surface of materials for LSBs.

## 2.2. Conductivity enhancement

The conductivity of sulfur host plays a pivotal role in sulfur cathode performance, which not only influences electron transport, but also tightly relates to redox kinetics of the Li–S system. If the sulfur host materials are electrical insulators, the adsorbed LiPSs may not be reduced despite off bound to the host.<sup>43</sup> Zhang<sup>44</sup> studied the relationship between the electrical conductivity of polar host materials and the redox kinetics of electrochemical reactions. The results show that conductive polar TiC increases the intrinsic activity for liquid–liquid LiPSs interconversion and liquid–solid precipitation of Li<sub>2</sub>S more than non-polar carbon and semiconductor TiO<sub>2</sub>.<sup>44</sup> Therefore, the host material must simultaneously possess interaction with LiPSs and conductivity, benefiting the homogeneous distribution of sulfur compounds,



and synergistically inhibiting the LiPSs shuttle and accelerating the reaction kinetics.<sup>43,45</sup> In comparison to metal oxides, the transition-metal sulfides usually exhibit higher conductivity, especially for CoS<sub>2</sub>, its electrical conductivity is up to  $6.7 \times 10^5 \text{ S cm}^{-1}$ ,<sup>24</sup> which is much higher than that of Co<sub>9</sub>S<sub>8</sub> ( $290 \text{ S cm}^{-1}$ ),<sup>5</sup> FeS ( $80 \text{ S cm}^{-1}$ ),<sup>46</sup> CuS ( $870 \text{ S cm}^{-1}$ ),<sup>47</sup> reduced graphene oxide ( $170 \text{ S cm}^{-1}$ )<sup>7</sup> and Ti<sub>4</sub>O<sub>7</sub> ( $3.2 \pm 0.1 \text{ S cm}^{-1}$ ).<sup>48</sup> Therefore, the transition-metal sulfides can improve the overall conductivity of the sulfur cathodes, simultaneously, nanostructured transition-metal sulfides are effective conductive polar host materials which can adsorb LiPSs efficiently and mitigate Li<sub>2</sub>S<sub>2</sub>/Li<sub>2</sub>S detaching from cathodes.<sup>5</sup> However, the electrical conductivity of transition-metal sulfides varies significantly. They can be classified as semimetals (CoS<sub>2</sub>)<sup>19</sup> and semiconductors (FeS<sub>2</sub>).<sup>33</sup> Therefore, the selection of metal sulfides based on conductivity should be considered when designing sulfur host materials for LSBs.

### 2.3. Catalytic effect on the redox of sulfur species

Besides the strong chemical interaction with LiPSs, transition-metal sulfides provide some catalytic effect on the redox of LiPSs. Through accelerating the conversion of LiPSs, their diffusion to electrolyte is relieved and kinetic barriers are effectively overcome.<sup>18</sup> As a result, the battery performance is improved, including lower polarization, higher Coulombic efficiency, excellent cycling stability and rate performance. The redox peaks of Co<sub>3</sub>S<sub>4</sub>-S shifted towards the quasi-equilibrium potentials and plateau gap of charge-discharge process were narrowed, due to faster redox kinetic than the pristine sulfur cathode.<sup>24</sup> To further testify the enhanced reaction kinetics, a symmetric cell (Fig. 3(a)) was constructed

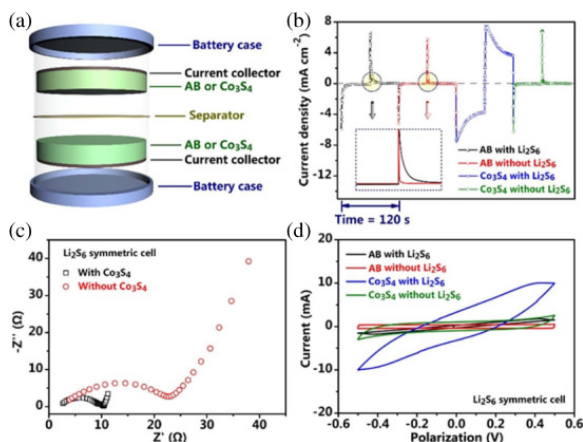


Fig. 3. (a) Schematic of a symmetric cell. (b) Chronoamperometric curves, (c) EIS plots, and (d) CV profiles of the Li<sub>2</sub>S<sub>6</sub> and AB symmetric cells.<sup>24</sup>

with Co<sub>3</sub>S<sub>4</sub> electrodes. As demonstrated in Fig. 3(b), the current response of Co<sub>3</sub>S<sub>4</sub> and acetylene black (AB) cells both become much higher after the addition of Li<sub>2</sub>S<sub>6</sub>. And the Co<sub>3</sub>S<sub>4</sub> cell possesses much smaller semicircle reaction than the AB cell, as shown in Fig. 3(c), indicating the electrode reaction kinetics improves. Meanwhile, the Co<sub>3</sub>S<sub>4</sub> cell reveals higher current responses than the AB cell in Li<sub>2</sub>S<sub>6</sub>-containing electrolyte, as shown in Fig. 3(d). It can be concluded that Co<sub>3</sub>S<sub>4</sub> can adsorb sulfur species, simultaneously enhancing the redox reaction kinetics of LiPSs.<sup>24</sup> A similar result was obtained when sulfides were added into sulfur cathode, such as CoS<sub>2</sub>,<sup>19</sup> WS<sub>2</sub>.<sup>35</sup> A series of transition-metal sulfides were studied by Cui to investigate the factors determining the sulfur conversion chemistry.<sup>28</sup> The S@G/CNT cathode with the addition of VS<sub>2</sub>, CoS<sub>2</sub> and TiS<sub>2</sub> demonstrate faster Li<sup>+</sup> diffusion and better reaction kinetics than those of Ni<sub>3</sub>S<sub>2</sub>, SnS<sub>2</sub> and FeS (Figs. 4(a)–4(c)), indicating high catalytic activity for sulfur conversion reaction. The diffusion barriers for Li<sup>+</sup> on Ni<sub>3</sub>S<sub>2</sub>, TiS<sub>2</sub>-containing cathodes show better reaction kinetics: a lower barrier endows faster Li<sup>+</sup> diffusion rate on the surface of the host materials, making redox reaction between lithium and sulfur facilitated. As a result, the cathodes containing VS<sub>2</sub>, TiS<sub>2</sub> and CoS<sub>2</sub> with higher binding energy and lower Li<sup>+</sup> diffusion and activation energy barriers, deliver better capacity and cycling stability (Fig. 4(e)).

Besides the catalysis for liquid-liquid transformation of LiPSs, transition-metal sulfides promote the liquid-solid conversion process, namely, the reaction of LiPSs to Li<sub>2</sub>S and

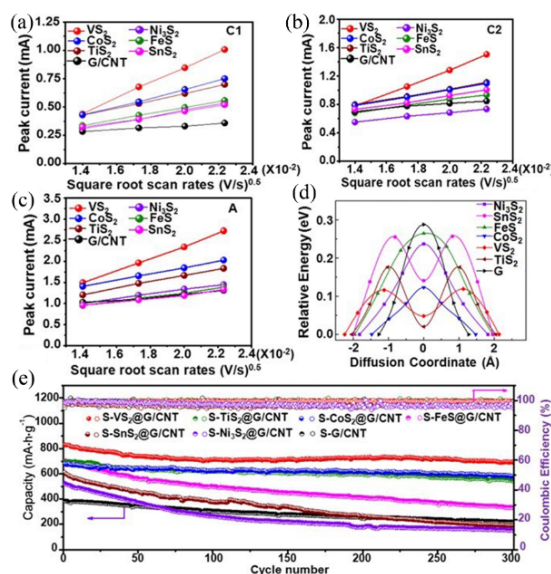


Fig. 4. Diffusion behaviors of Li<sup>+</sup> on the surface of graphene and Ni<sub>3</sub>S<sub>2</sub>, SnS<sub>2</sub>, FeS, CoS<sub>2</sub>, VS<sub>2</sub>, TiS<sub>2</sub>: (a) plots of first CV reduction peak current (I<sub>C1</sub>: S<sub>8</sub> → LiPSs), (b) plots of second CV reduction peak current (I<sub>C2</sub>: LiPSs → Li<sub>2</sub>S<sub>2</sub>/Li<sub>2</sub>S), and (c) plots of CV oxidation peak current (I<sub>A</sub>: Li<sub>2</sub>S<sub>2</sub>/Li<sub>2</sub>S → S<sub>8</sub>) vs. the square root of the scan rates. (d) Energy profiles of Li<sup>+</sup> diffusion behaviors on graphene and different metal sulfides. (e) Cycling stability and corresponding Coulombic efficiency at 0.5 C for 300 cycles.<sup>28</sup>

vice versa. rGO–VS<sub>2</sub> is abundant in active sites for the formation of Li<sub>2</sub>S. Furthermore, it also accelerates the conversion from Li<sub>2</sub>S to LiPSs.<sup>36</sup> In contrast to the cycled rGO/S cathode with a clean rGO surface and irregular Li<sub>2</sub>S particles, the cycled rGO–VS<sub>2</sub>/S exhibited Li<sub>2</sub>S uniformly deposited on the rGO–VS<sub>2</sub> without bulk Li<sub>2</sub>S particles.

The catalysis of sulfides for LiPSs conversion is closely related to their conductivity and the polar interactions with LiPSs. Upon cycling, when LiPSs maintain close electrical contact with host materials with strong chemical interaction, low resistance of electron transfer and fast kinetics of LiPSs conversion process may be really realized. The structure, stability and behavior of solvent solvated-Li<sup>+</sup> influences the behavior of the anions in the Li–S redox reactions. And the stability of the major polysulfide intermediates (S<sub>4</sub><sup>2-</sup> in DOL: DME) can improve the reaction rates of the LSBs.<sup>49</sup> And Warburg impedance is associated with the diffusion of Li<sup>+</sup> in the bulk of the electrode material, the larger Li<sup>+</sup> diffusion coefficient, the smaller Warburg factor values.<sup>50</sup> Additionally, strong interaction of transition-metal sulfides with LiPSs leads to relatively low LiPSs viscosity in the electrolyte, inducing relatively fast Li<sup>+</sup> diffusion. Moreover, fast Li<sup>+</sup> diffusion rate facilitates the sulfur transformation chemistry on the surface of transition-metal sulfides.<sup>28</sup> Therefore, the electron conductivity and ion diffusion should be as high as possible in the designed cathode, and strong interaction should be simultaneously taken into consideration, to maximize the catalytic effect of LiPSs. However, the mechanisms of fast kinetics is not only related to electronic conductivity enhanced by the transition-metal sulfides with excellent conductivity.<sup>24</sup> Although transition-metal sulfides have been proved to exhibit catalytic effect on the LiPSs conversion, its catalytic mechanism and further improvement have not been discerned clearly. MoS<sub>2</sub> with a controlled amount of sulfur deficiency (MoS<sub>2-x</sub>/rGO) was synthesized to catalyze the LiPSs conversion in a sulfur cathode. The CV peaks and peak separation in the MoS<sub>2-x</sub>/rGO cell were significantly narrowed than that of the MoS<sub>2</sub>/rGO (without sulfur deficiency) and the rGO cells. Furthermore, it was demonstrated that for LiPSs transformation, more electrochemically active sites existed on the MoS<sub>2-x</sub>/rGO surface compared to rGO, confirming sulfur deficiencies got involved in the LiPSs conversion and greatly facilitated the LiPSs redox.<sup>51</sup> This provides method strategy for improving the catalytic effect of sulfides.

## 2.4. Sulfur-equivalent cathode or co-cathode

Sulfur-equivalent cathode was proposed by Li,<sup>52</sup> for instance, MoS<sub>3</sub> was used as cathode instead of sulfur. The MoS<sub>3</sub> delivered an initial specific capacity of 667 mAh g<sup>-1</sup> based on MoS<sub>3</sub> mass, and 1482 mAh g<sup>-1</sup> based on the sulfur mass

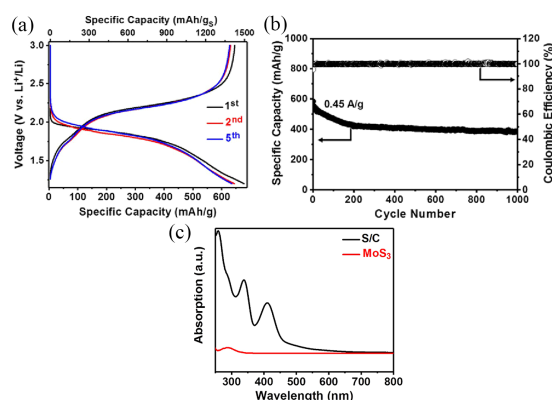


Fig. 5. Electrochemical performances of MoS<sub>3</sub> as the sulfur-equivalent cathode for LSBs. (a) Galvanostatic charge-discharge profiles at 23 mA g<sup>-1</sup>; specific capacity was based on the mass of sulfur in MoS<sub>3</sub> (top x-axis) or the total mass of MoS<sub>3</sub> (bottom x-axis). (b) Cycling performance and Coulombic efficiency at 0.45 A g<sup>-1</sup>; (c) UV-Vis adsorption spectrum of the electrolyte of the Li-MoS<sub>3</sub> battery after 100 cycles comparing with that of conventional LSBs after 100 cycles.<sup>52</sup>

(Fig. 5(a)). It exhibited excellent cycling stability, and remained 383 mAh g<sup>-1</sup> after 1000 cycles (Fig. 5(b)), due to the free of LiPSs (Fig. 5(c)). NiS was also employed as cathode with LiTFSI electrolyte for lithium batteries, and oxidation peaks and reduction peaks were observed at 1.2–1.3 V and 1.9–2.1 V, respectively, corresponding to the redox reactions of NiS. The NiS electrode exhibited the initial discharge capacities of 300 mAh g<sup>-1</sup>, 450 mAh g<sup>-1</sup> and 550 mAh g<sup>-1</sup> at C/10, C/20 and C/50, respectively. And the fading rate was only 23% at C/6 after 100 cycles.<sup>53</sup> Similarly, NiS<sub>2</sub>/FeS holey film cathode exhibited an excellent discharge capacity of 580 mAh cm<sup>-3</sup> and a low capacity fading.<sup>46</sup>

TiS<sub>2</sub> was composited with carbon additives as a co-cathode material of LSBs. TiS<sub>2</sub> also suffers redox reaction with lithium, and contributed 252 mAh g<sup>-1</sup> more than the pristine sulfur electrode (1082 mAh g<sup>-1</sup>), because TiS<sub>2</sub> facilitates the dispersion and utilization of active material sulfur as well as stabilizes the cathode structure.<sup>54</sup> However, not all sulfides can be used as sulfur-equivalent cathode or co-cathode materials. For example, Co<sub>9</sub>S<sub>8</sub> only exhibits a capacity of 15–35 mAh g<sup>-1</sup> in the typical LSB voltage window.<sup>21</sup> MoS<sub>2</sub> has almost no capacity, because lithiation of MoS<sub>2</sub> occurs below 1.5 V vs. Li/Li<sup>+</sup>, which is lower than the voltage window of LSBs.<sup>51,55</sup>

## 2.5. Tap density improvement

In the face of practical application for LSBs, gravimetric energy density is also inevitable to be investigated, especially when current collector, conductive additive and binder are considered.<sup>56</sup> Additionally, thick electrode, long electron pathway and poor volumetric capacity are also thorny issues caused by sulfur host materials with low tap density.<sup>57,58</sup>

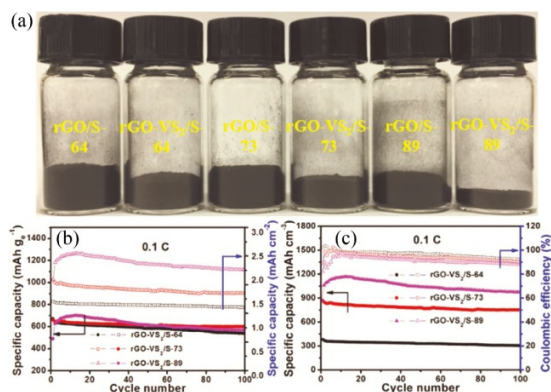


Fig. 6. (a) Volume comparison of rGO/S and rGO-VS<sub>2</sub>/S with the same mass. (b) The mass/areal capacity of rGO-VS<sub>2</sub>/S at 0.1 C, (c) the volumetric capacity and Coulombic efficiency of rGO-VS<sub>2</sub>/S at 0.1 C.<sup>36</sup>

More attention has been paid to high-volume energy density for LSBs, which is a key factor when applied in compact space.<sup>59</sup> In recent years, great achievements have been made in promoting the cathode properties and tap density with transition-metal compounds in LSBs.<sup>17</sup> Transition-metal sulfides hold the great promise to obtain packed electrodes for LSBs with excellent volumetric energy density due to its high tap density, which is much higher than porous carbon.<sup>20</sup> The volume of rGO-VS<sub>2</sub>/S samples are much smaller compared to rGO/S with the same sulfur content (Fig. 6(a)), obviously enlarging the sample density only with 5 wt.% VS<sub>2</sub>. As demonstrated in Fig. 6(b), rGO-VS<sub>2</sub>/S-64, rGO-VS<sub>2</sub>/S-73 and rGO-VS<sub>2</sub>/S-89 delivers the maximal discharge capacities of 660.0, 675.0 and 721.5 mAh g<sup>-1</sup>, respectively, in which the mass of conductive additive and binder are also included, and their corresponding areal discharge capacities are 1.45, 2.00 and 2.60 mAh cm<sup>-2</sup>, respectively. Additionally, the volumetric discharge capacity of rGO-VS<sub>2</sub>/S-89 can reach up to 1182.1 mAh cm<sup>-3</sup>, based on the total volume including every component inside the battery (Fig. 6(c)). By contrast, rGO/S-64 only exhibits the volumetric capacity of 194.6 mAh cm<sup>-3</sup>, which is far inferior to that of rGO-VS<sub>2</sub>/S-64.<sup>36</sup> In addition to its effect on volumetric capacity, area-specific capacity has also been promoted. Extremely high areal mass loading of sulfur even reached 40 mg cm<sup>-2</sup> with high areal capacity and high specific capacity using S<sub>8</sub>/TiS<sub>2</sub> hybrid foam as sulfur cathode, benefitting from its high conductivity and strong affinity for LiPSs.<sup>56</sup>

### 3. Conclusions and Outlook

Combining the chemical adsorption, conductivity enhancement and catalytic effect, transition-metal sulfides can promote whole solid-liquid-solid redox kinetics of sulfur cathode, thus delivering high specific capacity, excellent cycling stability as well as rate capability. And there is a close

relationship between these aspects. The strong interaction maintains electrical contact of the LiPSs with transition-metal sulfides and accelerates electron transfer, thus rendering the catalytic effect of transition-metal sulfides. Simultaneously, the catalysis itself is closely related to electron transfer. Therefore, the strong interaction and high conductivity positively promotes the catalytic effect of transition-metal sulfides for LiPSs conversion. As a result, the polar interaction with LiPSs and its conductivity may be considered firstly, and the catalytic effect is also considered for enhancing cathode performance of LSBs. Furthermore, the relationship between the catalytic mechanism of transition-metal sulfides and the chemical bonding has been challenged for further studies.

Despite the merits of sulfides as mentioned above, their inherent defects determine that they are fit for applying as additive of other host materials for sulfur cathodes, especially due to their poor surface area and low pore volume. In addition, the obtained sulfides are usually large particles, thus only limited active sites of affinity and catalysis for LiPSs. Consequently, sulfides are often composited with other sulfur host materials, such as carbon nanotube and graphene, to improve surface area, conductivity and physical confinement. Additionally, structural design is quite essential for achieving synergistic effect to improve cathode performance of LSBs. As for the structural design, nanocrystallization and quantization is an effective approach to enlarge surface and increase the active sites. Sulfides-embedded carbon polyhedron composites, which are synthesized using metal organic framework materials as precursor and template, may be ideal composites for sulfur host. The reserved structure with enough void space not only ensures the sulfur loading and accommodate the volume changes during the cycles, but also ensures uniform dispersion of transition-metal sulfides. All in all, to rationally design and utilize transition-metal sulfides may suppress the LiPSs shuttling and accelerate the reaction of sulfur species in LSBs, but it has been challenging. Some future works are required to address the catalyze mechanism of transition-metal sulfides for LSBs.

### References

1. X. L. Ji, K. T. Lee and L. F. Nazar, *Nat. Mater.* **8**, 500 (2009).
2. Y. X. Yin *et al.*, *Angew. Chem. Int. Ed.* **52**, 13186 (2013).
3. A. Manthiram *et al.*, *Chem. Rev.* **114**, 11751 (2014).
4. J. Q. Huang *et al.*, *ACS Nano* **9**, 3002 (2015).
5. X. Liu *et al.*, *Adv. Mater.* **29**, 1601759 (2017).
6. Q. Pang *et al.*, *J. Electrochem. Soc.* **162**, A2567 (2015).
7. Z. Y. Wang *et al.*, *Nat. Commun.* **5**, 5002 (2014).
8. D. W. Wang *et al.*, *J. Mater. Chem. A* **1**, 9382 (2013).
9. M. P. Yu *et al.*, *Energy Storage Mater.* **1**, 51 (2015).
10. P. Han and A. Manthiram, *J. Power Sources* **369**, 87 (2017).
11. Y. B. He *et al.*, *Dalton Trans.* **47**, 6881 (2018).

12. Y. C. Hao *et al.*, *ACS Appl. Mater. Inter.* **9**, 40273 (2017).
13. N. N. Hu *et al.*, *ACS Appl. Mater. Inter.* **10**, 18665 (2018).
14. G. Y. Zheng *et al.*, *Nano Lett.* **13**, 1265 (2013).
15. Z. P. Zeng and X. B. Liu, *Adv. Mater. Inter.* **5**, 1701274 (2017).
16. A. Eftekhari and D. W. Kim, *J. Mater. Chem. A* **5**, 17734 (2017).
17. X. X. Gu and C. Lai, *J. Mater. Res.* **33**, 16 (2018).
18. S. H. Yu *et al.*, *Accounts Chem. Res.* **51**, 273 (2018).
19. D. H. Liu *et al.*, *Adv. Sci.* **5**, 1700270 (2018).
20. Z. Yuan *et al.*, *Nano Lett.* **16**, 519 (2015).
21. Q. Pang, D. Kundu and L. F. Nazar, *Mater. Horiz.* **3**, 130 (2016).
22. Z. Li *et al.*, *ACS Appl. Mater. Inter.* **9**, 38477 (2017).
23. G. M. Zhou *et al.*, *ACS Nano* **7**, 5367 (2013).
24. J. Pu *et al.*, *Nano Energy* **37**, 7 (2017).
25. J. Zhou *et al.*, *Electrochim. Acta* **218**, 243 (2016).
26. C. Ye *et al.*, *Adv. Funct. Mater.* **27**, 1702524 (2017).
27. G. M. Zhou *et al.*, *Proc. Natl. Acad. Sci. USA* **114**, 840 (2017).
28. M. Li *et al.*, *Mater. Res. Bull.* **96**, 509 (2017).
29. D. Q. He *et al.*, *J. Electrochem. Soc.* **164**, A1499 (2017).
30. Z. L. Ma *et al.*, *J. Power Sources* **325**, 71 (2016).
31. S. S. Zhang and D. T. Tran, *J. Mater. Chem. A* **4**, 4371 (2016).
32. Y. Lu *et al.*, *Nanoscale* **8**, 17616 (2016).
33. J. Park *et al.*, *Adv. Energy Mater.* **7**, 1602567 (2017).
34. X. L. Li *et al.*, *J. Alloys Compd.* **692**, 40 (2017).
35. Z. B. Cheng *et al.*, *Adv. Energy Mater.* **8**, 1702337 (2018).
36. Z. W. Seh *et al.*, *Nat. Commun.* **5**, 5017 (2014).
37. T. Chen *et al.*, *Nano Energy* **38**, 239 (2017).
38. W. Liu *et al.*, *Proc. Natl. Acad. Sci.* **114**, 3578 (2017).
39. T. Chen *et al.*, *Nano Energy* **38**, 239 (2017).
40. P. Q. Guo *et al.*, *Electrochim. Acta* **256**, 28 (2017).
41. H. T. Wang *et al.*, *Nano Lett.* **14**, 7138 (2014).
42. K. Liang *et al.*, *Adv. Energy Mater. Lett.* **7**, 1701309 (2017).
43. H. J. Peng and Q. Zhang, *Angew. Chem. Int. Ed.* **54**, 11018 (2015).
44. H. J. Peng *et al.*, *Angew. Chem. Int. Ed.* **55**, 12990 (2016).
45. C. J. Hart *et al.*, *Chem. Commun.* **51**, 2308 (2015).
46. K. Liang *et al.*, *Adv. Energy Mater.* **7**, 1701309 (2017).
47. B. Jache *et al.*, *J. Power Sources* **247**, 703 (2014).
48. Q. Pang *et al.*, *Nat. Commun.* **5**, 4759 (2014).
49. Q. Zou and Y. C. Lu, *J. Phys. Chem. Lett.* **7**, 1518 (2016).
50. C. J. Tang *et al.*, *Adv. Funct. Mater.* **28**, 1704561 (2018).
51. H. B. Lin *et al.*, *Energy Environ. Sci.* **10**, 1476 (2017).
52. H. L. Ye *et al.*, *Proc. Natl. Acad. Sci. USA* **114**, 13091 (2017).
53. T. S. Sonia *et al.*, *Ceram. Int.* **40**, 8351 (2014).
54. Y. S. Su and A. Manthiram, *J. Power Sources* **270**, 101 (2014).
55. J. B. Ye *et al.*, *Electrochim. Acta* **190**, 538 (2016).
56. L. Ma *et al.*, *J. Mater. Chem. A* **3**, 19857 (2015).
57. D. Lin *et al.*, *Energy Environ. Sci.* **8**, 2371 (2015).
58. Z. H. Liu *et al.*, *Energy Storage Mater.* **13**, 112 (2018).
59. X. F. Yang *et al.*, *Electrochem. Energ. Rev.* **1**, 1 (2018).